Linear and Nonlinear Susceptibilities of a Decoherent Two Level System

Gregory Levine
Department of Physics, Hofstra University, Hempstead, NY 11550
and
Department of Physics, Brookhaven National Laboratory, Upton, NY 11973-5000
(February 1, 2008)

The linear and nonlinear dynamical susceptibilities of a two level system are calculated as it undergoes a transition to a decoherent state. Analogously to the Glover-Tinkham-Ferrell sum rule of superconductivity, spectral weight in the linear susceptibility is continuously transferred from a finite frequency resonance to nearly zero frequency, corresponding to a broken symmetry in the thermodynamic limit. For this reason, the behavior of the present model (the Mermin Model) differs significantly from the spin-boson model. The third order nonlinear susceptibility, corresponding to two-photon absorption, has an unexpected non-monotonic behavior as a function of the environmental coupling, reaching a maximum within the decoherent phase of the model. Both linear and nonlinear susceptibilities may be expressed in a universal form.

PACS numbers: 03.65.Bz, 42.50.-p, 42.50.Lc, 42.65.-k

I. INTRODUCTION

A vast body of work has been devoted to understanding the transition to decoherence in models of a two-level-system (TLS) coupled to an infinite set of environmental degrees of freedom [1]. The central quantity in this transition is the dynamical correlation function, or equivalently, the linear susceptibility, $\chi''(\nu)$, of the system degrees of freedom. To our knowledge, no studies of the nonlinear susceptibility have been undertaken. Our interest in the nonlinear response is twofold: 1) experimental probes of Macroscopic Quantum Coherence (MQC) might access the nonlinear regime and 2) the nonlinear susceptibility appears to bear a different relationship to the coherence of the TLS than the linear susceptibility. A measure of coherence of the system is the quantity of spectral weight within the resonance peak of $\chi''(\nu)$ associated with the TLS—this is simply proportional to the probability of absorbing a *single* photon. Absorption of a photon at a precise energy is a property uniquely associated with the underlying coherence of the quantum mechanical system. As the coupling to the environment is increased and the system increasingly localizes in one state, the probability of single photon absorption diminishes. In this paper we address whether *two photon* absorption is qualitatively similar—is it similarly linked to the underlying coherence of the system? We are thus led to the study of nonlinear susceptibilities of a TLS as the system is tuned through a decoherence transition.

N. D. Mermin investigated a model obtained from the well known spin-boson Hamiltonian by keeping only the lowest two levels of each harmonic oscillator comprising the environmental bath [2]. The Hamiltonian therefore contains a "system" spin-1/2, represented by the Pauli matrices σ, coupled to a set of N "environment" spin-1/2 degrees of freedom, $\{\mathbf{s}_j\}$. The resulting Hamiltonian

$$H = \frac{t}{2}\sigma_x + \frac{\lambda}{4N}\sigma_z \sum_{j=1}^{N} (s_j^+ + s_j^-) + \frac{\omega}{2N}\sum_{j=1}^{N} s_j^z \qquad (1)$$

(henceforth referred to as the Mermin Model) can be solved to demonstrate the close correspondence between decoherence and a second order phase transition. The transition in the Mermin model also bears some similarity to the decoherence transition in the Ohmic case of the spin-boson Hamiltonian [3]. Owing to its finite Hilbert space, exact dynamical susceptibilities (linear and nonlinear) can be calculated and followed through the transition. The finite dimensionality may also be realistic in some physical settings and exhibits the expected corrections to an "infinite environment" thermodynamic phase transition. In this paper, we will present such calculations and a careful study of the Mermin Model at the linear level, demonstrating an analogy to the superconducting transition in the "dirty" limit. We will then go on to the calculation and interpretation of the third order, nonlinear susceptibility corresponding to two photon absorption.

To briefly summarize our findings: The transition to decoherence is induced by strong coupling to environmental degrees of freedom (large λ) or a small system energy scale (small t). Below a critical coupling, λ_c, all spectral weight of the dynamical susceptibility

$$\chi''(\nu) \equiv \mathrm{Im}\ \frac{i}{4}\int_{-\infty}^{\infty} dt \langle 0|[\sigma(t),\sigma(0)]|0\rangle \theta(t) e^{i\nu t} \qquad (2)$$

lies in the principal resonance of the TLS at an energy t. When the coupling is increased above the critical coupling, a new exponentially small energy scale $O(te^{-N/2})$ emerges, associated with a broken symmetry, $\langle\sigma\rangle \neq 0$, in the thermodynamic limit $N \to \infty$. This feature corresponds to tunneling modified by a Franck-Condon

type overlap factor. As the coupling is increased, spectral weight is continuously shifted to the "near-zero" frequency channel. The weight of the delta-function, $\delta(0^+)$, is simply the order parameter, $|\langle 0|\sigma|0\rangle|^2$ (or, more exactly, $|\langle 1|\sigma|0\rangle|^2$, for large but finite N). However, the dynamical susceptibility obeys a sum rule implying that an incompletely formed broken symmetry state leaves some spectral weight at the position of the principal resonance, set by t.

It is in this respect that the Mermin model differs from the ohmic case of the spin-boson Hamiltonian (SBH). In the SBH, the Toulouse limit (at $\alpha = 1/2$), corresponding to complete inelastic broadening of the resonance, is a precursor to localization of the system spin (at $\alpha = 1$) [4,5]. In the Mermin model, the quantum resonance of the system spin—although damped—remains intact through the decoherence transition. This behavior is analogous to the Glover-Tinkham-Ferrell [6] sum rule for the dynamical conductivity in superconductors. Spectral weight falling in the gap region, proportional to the superfluid density (or, equivalently, the order parameter) is redistributed to a delta-function at zero frequency. In the case of the transition to decoherence, finite but supercritical coupling, $\lambda > \lambda_c$, is analogous to the transition to superconductivity in the dirty limit where the superconductor can absorb energy above the gap.

In contrast, the nonlinear response has a more complicated behavior. Two photon absorption (TPA) requires the presence of ancillary levels as intermediate states and is therefore enhanced when there is some degree of "inelastic" broadening of the primary resonance. At the two extremes, TPA is zero when $\kappa > \kappa_c$ and the environment is decoupled from the system—but it is also zero when $\kappa \to 0$ and the system is completely decoherent.

We now turn to a review of the analytical results obtained from the Mermin model.

II. THE MERMIN MODEL

In the absence of coupling to the environment, the two level system in (1) possesses a ground state in a coherent superposition of spin up and spin down (denoted $|+\rangle - |-\rangle$) and will display a sharp resonance in $\chi''(\nu)$ at $\nu = t$. When environmental coupling is included, there are two effects commonly associated with decoherence. First, the coherence features should shift to lower frequency (Franck-Condon overlap) and secondly, the peak should broaden from "inelastic" energy exchange with the environment. These two effects are nicely demonstrated in the Mermin Model. In (1), the environment spins may be summed to one big $O(N)$ spin, $\mathbf{S}$, and the Hamiltonian becomes

$$H = \frac{t}{2}\sigma_x + \frac{\lambda}{2N}\sigma_z S_x + \frac{\omega}{2N} S_z \tag{3}$$

As Mermin points out, the advantage of the Hamiltonian (3) is that in the limit $N \to \infty$, the environment spins may be replaced in the Hamiltonian by the x and z components of a classical spin angular momentum: $\frac{\lambda}{N}\sigma_z S_x \to \frac{1}{2}\lambda\sigma_z \sin\theta$ and $\frac{\omega}{N} S_z \to -\frac{1}{2}\omega\cos\theta$. The resulting Hamiltonian

$$H = \frac{t}{2}\sigma_x + \frac{\lambda}{4}\sigma_z \sin\theta - \frac{\omega}{4}\cos\theta \tag{4}$$

may be diagonalized and its ground state eigenvalue, $E_0(\theta)$, given by

$$E_0(\theta) = -\frac{1}{2}\sqrt{t^2 + \frac{\lambda^2}{4}\sin^2\theta} - \frac{\omega}{4}\cos\theta \tag{5}$$

minimized with respect to θ.

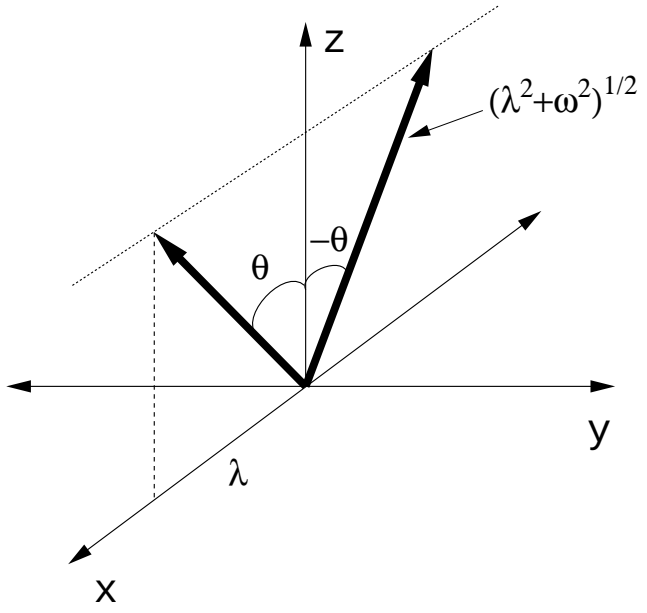

Figure 1

FIG. 1. The classical ($N \to \infty$) minimum energy configurations of the environment (solid black arrows) in the strongly coupled phase, $\kappa < \kappa_c$. ($\kappa \equiv 2\omega t/\lambda^2$; $\kappa_c \equiv 1$).

The critical behavior of the model may now be seen by examining the ground state energy E_0, as function of t. E_0 bifurcates at a finite value of t going from a singlet, non-degenerate root for $t > \lambda^2/2\omega$ to a doubly degenerate set for $t < \lambda^2/2\omega$.

$$\theta_0 = 0 \qquad t > \lambda^2/2\omega \tag{6}$$

$$\sin\theta_0 = \pm\sqrt{\frac{1 - 4t^2\omega^2/\lambda^4}{1 + \omega^2/\lambda^2}} \qquad t < \lambda^2/2\omega \tag{7}$$

In the former case, the environment is decoupled from the system and always points along the z-axis to minimize its

"Zeeman" energy corresponding to the last term of (3). In the latter case, the environment and the system spins are frozen in two distinct orientations with degenerate energies. The ground state wave function is still in a superposition $\alpha|+\rangle - \beta|-\rangle$ but it is no longer an evenly weighted one ($\alpha = \beta$); rather, the two roots correspond to the system predominantly in $|+\rangle$ or $|-\rangle$.

However, for finite (even very large) N, the system must be in an evenly weighted superposition—independent of the value of t. For $t \to 0$, it is possible to estimate the tunnel splitting between the ground and first excited states. Following [2], we consider the adiabatic environment (or small t) limit in which the environment instantaneously adjusts to the localization of the system in a given state and thus "points" at the angle θ_0, as shown in Fig. 1. For the system to jump to the other state, the environment must be caught in a fluctuation which points along the other direction, $-\theta_0$. The amplitude for N spin-1/2's to be found at an angle $2\theta_0$ away is $\cos^N \theta_0$. The new tunnel splitting is thus reduced by a Franck-Condon type overlap factor:

$$t^* = t\langle\theta_0|R_y(2\theta_0)|\theta_0\rangle = t\cos^N\theta_0 = t\frac{1}{(1+\lambda^2/\omega^2)^{N/2}} \tag{8}$$

where $R_y(2\theta_0)$ is the rotation operator. Note that this is still a purely conservative process; the resonance is perfectly sharp although at an exponentially reduced energy scale. We will refer to this resonance as the Franck-Condon resonance.

Although, for finite N and t, the symmetry is unbroken and the ground state is an evenly weighted superposition, there must be some symptom of the crisis at $t \sim \lambda^2/2\omega$ when N becomes large. Presumably, this symptom should be the inelastic broadening of the resonance to an over damped state. Following along the lines of the Fermi Golden Rule (FGR) calculation in [1], we treat the last two terms of (3) as the unperturbed Hamiltonian, H_0. H_0 is a Zeeman-like Hamiltonian with a magnetic field that depends upon the z-component of the system spin. Therefore it should be diagonalized with a σ_z dependent rotation about the y-axis:

$$R \equiv R_y(\sigma_z\theta_0) = e^{-i\sigma_z\theta_0 S_y} \tag{9}$$

The transformed Hamiltonian is then

$$H_0' = R^\dagger H_0 R = \frac{\omega}{2N}S_z\cos\theta_0(1+\frac{\lambda^2}{\omega^2}) \tag{10}$$

where $\tan\theta_0 = \lambda/\omega$ has been chosen to eliminate the S_x term in H_0'. Now turning to the first term of (3), the rotation yields:

$$H_1' \equiv \frac{t}{2}R^\dagger\sigma_x R = \frac{t}{2}(\sigma^+ e^{-i\sigma_z\theta_0 S_y} + \sigma^- e^{+i\sigma_z\theta_0 S_y}) \tag{11}$$

Now the system is prepared in a state $|+\rangle$ with the environment in its ground state $S_z = -N/2$ (which will be denoted $|-N/2\rangle$). The transition rate is now calculated by applying Fermi's Golden Rule, treating H_1' as the perturbation.

$$\Gamma = \frac{t^2}{4}\sum_{m=-N/2}^{N/2}|\langle -|\langle m|\sigma^- e^{+i\sigma_z\theta_0 S_y}|-N/2\rangle|+\rangle|^2\delta(E_f - E_i) \tag{12}$$

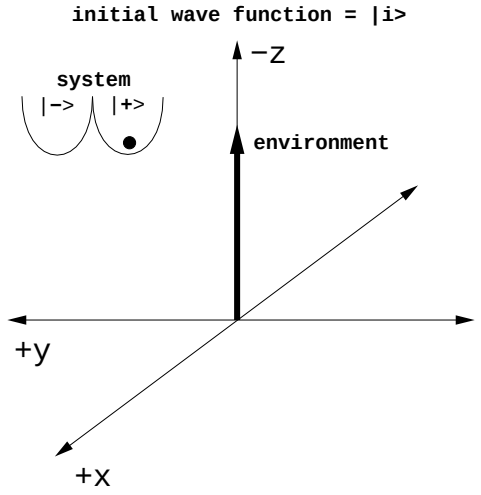

Figure 2a

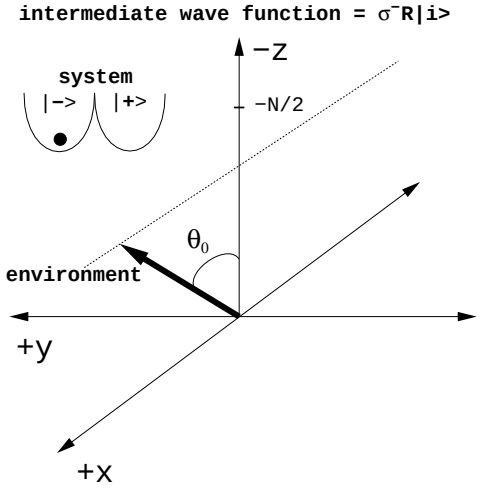

Figure 2b

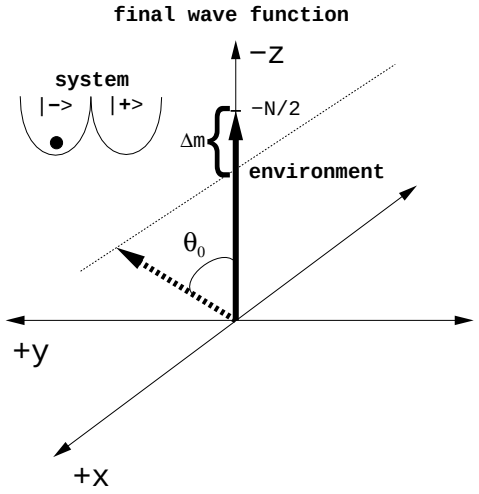

Figure 2c

FIG. 2. Sequence of states (a) initial, (b) intermediate and (c) final, depicting Fermi's Golden Rule applied to the Mermin Model. Solid black arrow is the environment; state of the system is shown in the upper left. Final environment state must make a fluctuation of approximately $\Delta m = -N/2\cos\theta_0 + N/2$ to have a reasonable overlap with the intermediate state. The system drives the environment to dissipate energy.

As depicted in Figs. 2(a-c), H_1' induces a rotation of the environment by $-\theta_0$ about the y-axis as the system flips from $|+\rangle$ to $|-\rangle$. Since the environment is now rotated away from the environment ground state of the *final* configuration ($\langle -|\langle -N/2|$) as well (Fig. 2c), the dominant contribution to Γ comes from an excited (rotated) final state. Looking at the geometry of Fig. 2c, the final state, $\langle -|\langle m = -N/2\cos\theta_0|$, contributes most strongly. Using the Hamiltonian H_0', the energy difference is computed:

$$\Delta E = E_f - E_i \sim \frac{\omega}{4}(1-\cos\theta_0)\cos\theta_0(1+\lambda^2/\omega^2) \sim \frac{\lambda^2}{8\omega} \tag{13}$$

This calculation suggests an interpretation of the earlier result (6) for the critical coupling obtained in the $N \to \infty$ limit. When the width of the resonance ΔE becomes comparable to t, the resonance is over damped and quantum coherence is destroyed.

Although both the adiabatic computation and the FGR one are small t perturbation theories and involve the same environment overlap amplitude, their interpretations are quite different. In the former, the system in the $|+\rangle$ state leaves an "imprint" upon the environment which, because it is nearly orthogonal to the imprint left by system state $|-\rangle$, reduces the tunneling amplitude by an exponentially small factor. The resonance must therefore shift from $O(t)$ to a smaller energy scale $O(te^{-N/2})$. In the latter case, the system forces the environment to dissipate energy and the resonance is broadened by $O(\lambda^2/\omega)$ but remains nominally at $O(t)$.

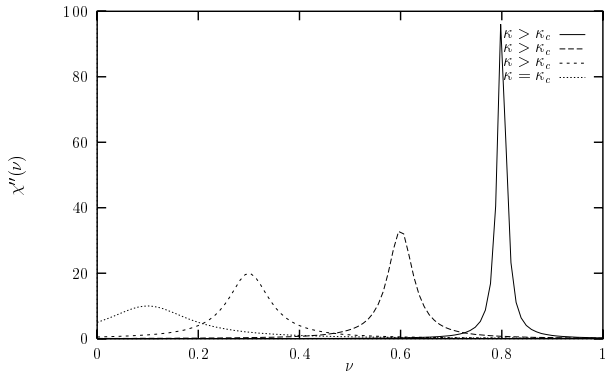

Figure 3

FIG. 3. Possible "continuous" evolution of spectral weight. The principal resonance and the Franck-Condon resonance are the same.

One might speculate upon two possible scenarios in which these two perturbative calculations are blended, as suggested in Figs. 3 and 4. In Fig. 3, a single resonance broadens and shifts to lower energy, decoherence occurring when the resonance becomes broadened beyond its energy scale. In this scenario, there is no explicit Franck-Condon energy scale, just the appearance of increasing spectral weight close to zero as the resonance becomes over-damped. In the other scenario, demonstrated in Fig. 4, spectral weight is only transferred to an exponentially small energy below some critical coupling; the resonance at t, although broadened, is not critically damped and remains distinct from the Franck-Condon resonance. To put it another way, the systems retains a gap of $O(t)$. Furthermore, even at finite N, there is essentially no "Franck-Condon effect" for $\kappa > \kappa_c$ (see Fig. 5). It is the second scenario that is manifested in the Mermin Model.

III. CALCULATIONS OF THE LINEAR SUSCEPTIBILITY: $\chi''(\nu)$

We consider the Hamiltonian (1) with an additional coupling to an external field $h(t) = h\cos\nu t$:

$$H_{\rm ext} = -h\frac{\sigma_z}{2}\cos\nu t \tag{14}$$

For calculating nonlinear susceptibilities it will be necessary to use explicitly real driving fields, so we adopt explicitly real notation for the expectation value of the

time dependent system spin, at this point. The time dependence of σ_z, at linear response, is

$$\frac{1}{2}\langle\sigma_z(t)\rangle = h\chi'(\nu)\cos\nu t - h\chi''(\nu)\sin\nu t \qquad (15)$$

At zero temperature, the response function $\chi(\nu)$ is given by the integral on the right hand side of (2). Expanded out,

$$\chi(\nu) = \frac{1}{\hbar}\sum_n \frac{1}{4}|\sigma_{0n}|^2\left(\frac{1}{\nu+\nu_{n0}-i\delta} - \frac{1}{\nu-\nu_{n0}-i\delta}\right) \qquad (16)$$

where $\nu_{ij} \equiv (E_i - E_j)/\hbar$ and $\delta = 0^+$. The matrix elements of the system spin $\sigma_{ij} \equiv \langle i|\sigma_z|j\rangle$ will be referred to as the order parameter matrix. (The state $|i\rangle$ now refers to the combined system and environment state.) Using (15), the rate of energy absorption is then

$$\Omega = -\frac{1}{2}\nu\chi''(\nu)h^2 \qquad (17)$$

Equations analogous to (15), (16) and (17) for the third order nonlinear susceptibility are derived in the Appendix.

The Hamiltonian (1) was diagonalized and the complete order parameter matrix, σ_{ij}, necessary for the linear and nonlinear calculations, was computed. It is natural to work with one dimensionless coupling constant, $\kappa \equiv 2\omega t/\lambda^2$. The critical coupling implied in the $N \to \infty$ calculation is then $\kappa = \kappa_c = 1$.

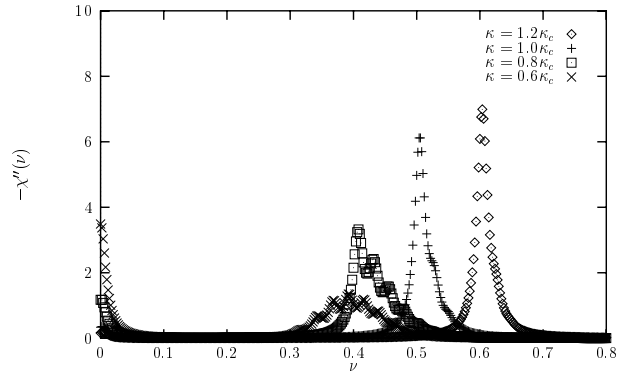

Figure 4

FIG. 4. Evolution of spectral weight in the Mermin Model. $\chi''(\nu)$ is shown for four values of κ decreasing below the critical value, κ_c. Despite some change in the position of the principal resonance, spectral weight emerges at $\nu \sim 0$ abruptly at κ_c and the two features remain distinct.

Fig. 4 shows the behavior of $\chi''(\nu)$ as the system energy scale t is reduced, corresponding to a range $\kappa = 0.6\kappa_c - 1.2\kappa_c$. These computations were performed for 80 environment spins. Computations with up to 300 environment spins suggest that there is little change beyond 80 spins. An artificial broadening ($\delta = 0.01$) was added to make the features more visible. As seen in this sequence, $\kappa = \kappa_c$ is marked by the appearance of the Franck-Condon resonance at an exponentially small energy scale ($\nu_{10} \sim 10^{-3}$). The spectral weight remaining at $O(t)$ when $\kappa > \kappa_c$ clearly exhibits inelastic broadening, although the resonance essentially disappears before becoming critically damped.

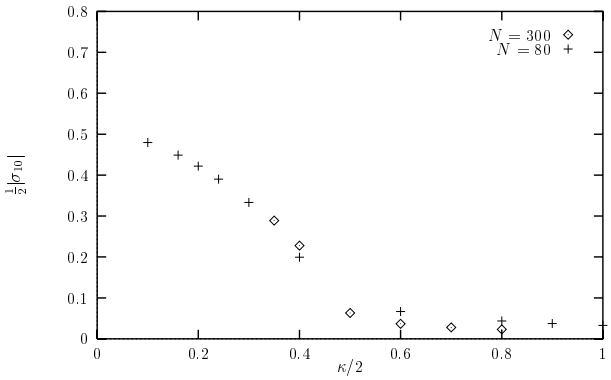

Figure 5

FIG. 5. The order parameter, σ_{10}, is plotted as a function of κ and exhibits second order phase transition behavior. κ was varied by changing t. Comparison of $N = 80$ and $N = 300$ data show the slope steepening at the critical point. When $\kappa > \kappa_c$, there is no weight in the Franck-Condon resonance other than that attributed to the rounding of the phase transition at finite N.

The counterpart, at finite N, to $\langle\sigma\rangle \neq 0$ at infinite N is the spectral weight at the Franck-Condon resonance, $\sigma_{10} \neq 0$. Fig. 5 demonstrates that σ_{10} behaves as expected in a second order phase transition; the slope at $\kappa = \kappa_c^+$ grows with increasing N. The matrix, σ_{ij}, and consequently, $\chi''(\nu)$, obey a sum rule:

$$\sum_i |\sigma_{ij}|^2 = 1 \qquad (18)$$

An incompletely developed broken symmetry ($|\sigma_{10}|^2 < 1$) means that spectral weight remains at the principal resonance at $O(t)$. This behavior is somewhat analogous to the superconducting transition and the Glover-Tinkham-Ferrell sum rule for the real part of the dynamical conductivity, $\sigma(\omega)$:

$$\int_0^\infty \sigma_{\rm n}(\omega)d\omega = \frac{\pi n_{\rm S} e^2}{2m} + \int_\Delta^\infty \sigma_{\rm S}(\omega)d\omega \qquad (19)$$

(Subscripts "n" and "s" refer to "normal" and "superconducting".) The sum rule states that spectral weight

missing from dynamical conductivity above the gap must reappear as superfluid (DC) Drude weight. This behavior may be compared with other models and computations of environmental spin decoherence [8]. These models differ from the Mermin Model in two respects: 1) typically the environmental coupling constant is comparable to the system energy scale instead of weak $O(\lambda/N)$ coupling, as in the present case; 2) the coupling between the system and environmental spins is isotropic, of the form, $\vec{\sigma}\cdot\vec{s}_j$. These differences lead to qualitatively different decoherence effects.

IV. NONLINEAR DYNAMICAL SUSCEPTIBILITY

In studying the nonlinear susceptibilities, we are interested in power absorption, as this is the relevant experimental probe for MQC. Consider the response of just a single two-level-system (TLS) coupled to ancillary levels: Driving the system with a signal at frequency ν results in third order nonlinear responses at ν and 3ν. The signal at 3ν is not absorptive and, in any case, would not be detected in any experimental setting where pumping and detection take place at (nearly) the same frequency. If the nominal frequency scale of the TLS is ν_0, there is an imaginary but *emissive* response at ν_0. (The non vanishing, odd order, nonlinear corrections to power absorption at ν_0 must alternate in sign to produce finite absorption at ν_0, consistent with the exact Rabi solution.) On the other hand, third order two-photon absorption (TPA) process at $\nu_0/2$ would resemble ordinary linear absorption of a $\nu_0/2$ TLS in that it would be detected as an absorptive phase shift when the pumping frequency reaches $\nu_0/2$. The reader is referred to ref. [7] for further details about nonlinear processes.

Fig. 6 shows the two photon absorption spectrum along with the linear susceptibility for several values of κ. Our basic result is the following: as the critical value of κ is reached and the two-level-system undergoes a transition to decoherence, the two photon absorption power, $\Omega_{2\gamma}$, begins to increase. It reaches a maximum at approximately $\kappa=\kappa_c/2$ and then decreases to zero as κ goes to zero. Fig. 7 shows the behavior of the TPA signal as a function of the control parameter κ.

The two photon absorption spectrum was calculated from an exact diagonalization of the Mermin model using the following expression for TPA (which is derived in the Appendix):

$$\begin{aligned}\Omega_{2\gamma} &= \frac{1}{2}h^4\nu\chi^{[3]}(\nu)\\ &= \frac{1}{8}(\frac{h}{2})^4\nu\frac{1}{\hbar^3}\sum_{nml}\sigma_{0n}\sigma_{nm}\sigma_{ml}\sigma_{l0}\\ &\quad\times P''_{0m}(-2\nu)P'_{l0}(\nu)P'_{n0}(\nu)\end{aligned}\tag{20}$$

In the expression above, the energy denominators have been abbreviated,

$$P_{ij}(\nu)\equiv\frac{1}{\nu-\nu_{ij}-i\delta}\tag{21}$$

To calculate (20) it is necessary to find all possible sets of four couplings that connect the ground state back to the ground state. These are referred to as "four link chains"; a few such chains are depicted in Fig. 8.

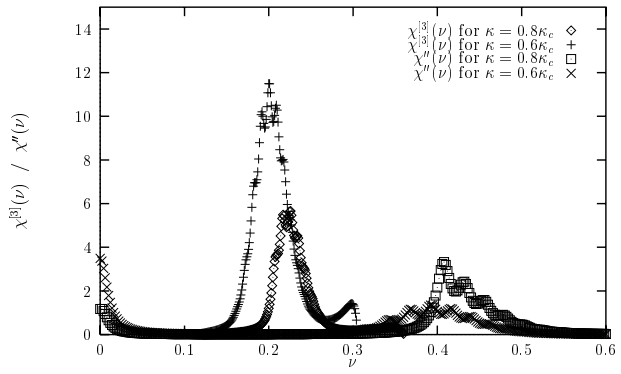

Figure 6

FIG. 6. Nonlinear susceptibilities for two photon absorption compared with the linear susceptibility for two values of κ. Note the increase in $\chi^{[3]}$ as κ is decreased from $0.8\kappa_c$ to $0.6\kappa_c$.

To understand the non-monotonic behavior of the TPA signal, we look at the expression (20). Isolating the absorptive pole, $\chi^{[3]}(\nu)$ can be factored in the following way:

$$\chi^{[3]}(\nu)=\frac{1}{4}(\frac{1}{2})^4\frac{1}{\hbar^3}\sum_m P''_{0m}(-2\nu)|\alpha_m(\nu)|^2\tag{22}$$

where $\alpha_m(\nu)$ is a sum over intermediate states,

$$\alpha_m(\nu)\equiv\sum_n\sigma_{0n}\sigma_{nm}P'_{n0}(\nu)=\sum_n\frac{\sigma_{0n}\sigma_{nm}}{\nu-\nu_{n0}}\tag{23}$$

$\alpha_m(\nu)$ is known in nonlinear optics literature as the degenerate hyperpolarizability. We focus our attention upon the *integrated* spectral weight, shown below for both linear and nonlinear susceptibilities ($\hbar=1$):

$$I_{\rm lin}=\int_{0^+}^{\infty}\chi''(\nu)d\nu\qquad I_{\rm nonlin}=h^2\int_{0^+}^{\infty}\chi^{[3]}(\nu)d\nu\tag{24}$$

The limits of integration are meant to restrict the integration to the principal resonance and exclude the contributions from the near degenerate ground states. (These

are the states $m = 0, 1$ excluded in the sum below.) The integrated weight is in some sense a "figure of merit" for detection of an MQC resonance. A meaningful comparison between linear and nonlinear absorption requires the multiplicative factor h^2 in the nonlinear expression. In both cases, the integration collapses the absorptive pole leaving, in the linear case,

$$I_{\rm lin} = \pi(\frac{1}{2})^2 \sum_{n\neq 1} |\sigma_{0n}|^2 = \pi(\frac{1}{2})^2(1-\sigma_{01}^2) \qquad (25)$$

and in the nonlinear case,

$$I_{\rm nonlin} = \pi h^2(\frac{1}{2})^4 \frac{1}{8} \sum_{m\neq 0,1} |\alpha_m(\nu_{m0})|^2 \qquad (26)$$

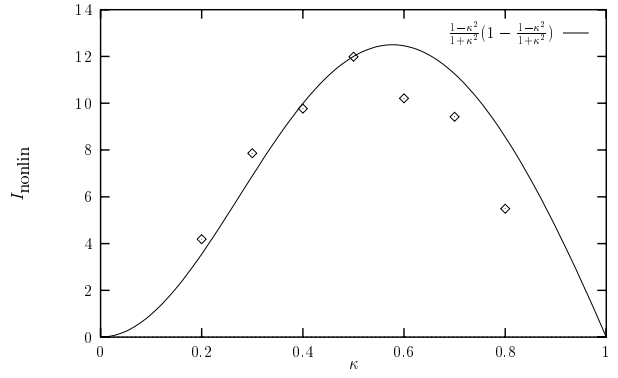

Figure 7

FIG. 7. Integrated spectral weight $I_{\rm nonlin}$ for two photon absorption as a function of κ. Solid line is the result of theory. The applied AC field strength $h = 1$.

Since $I_{\rm lin}$ given in equation (25) depends only upon the order parameter σ_{01}, it has a universal behavior in terms of κ through the decoherence transition (see equations (35), (36)). It turns out to be possible to express $I_{\rm nonlin}$ in a similar fashion within a simple approximation and understand the non-monotonic behavior seen in fig. 7. It will be shown that $I_{\rm nonlin}$ depends upon the order parameter through:

$$I_{\rm nonlin} = \frac{2\pi h^2}{\nu_0^2}(\frac{1}{2})^4\sigma_{01}^2(1-\sigma_{01}^2) + O(\frac{h^2\epsilon}{\nu_0^3}) \qquad (27)$$

and thus reaches a maximum at approximately $\kappa = \kappa_c/2$. (In the exact solution, $|\langle 0|\sigma_z|0\rangle|^2 \sim 1-\kappa^2$ for $\kappa_c = 1$; see equation (35).)

To understand this result, consider the usual conditions through which a broken symmetry is accessed mathematically: Apply a small static bias field $h_{\rm dc}$ coupled to the system through $H_{\rm dc} \equiv -h_{\rm dc}\sigma_z$ and take the limits in the order,

$$\lim_{h_{\rm dc}\to 0} \lim_{N\to\infty} \langle 0|\sigma_z|0\rangle \qquad (28)$$

In the decoherent phase ($\kappa < \kappa_c$), a field $h_{\rm dc} \sim O(te^{-N/2})$ will localize the system yielding $\langle 0|\sigma|0\rangle \neq 0$, but will have essentially no effect in the coherent phase ($\kappa > \kappa_c$). The relevant energy levels now look like the right half of Fig. 8 (the quasi-degenerate ground state levels are no longer coupled through σ_z).

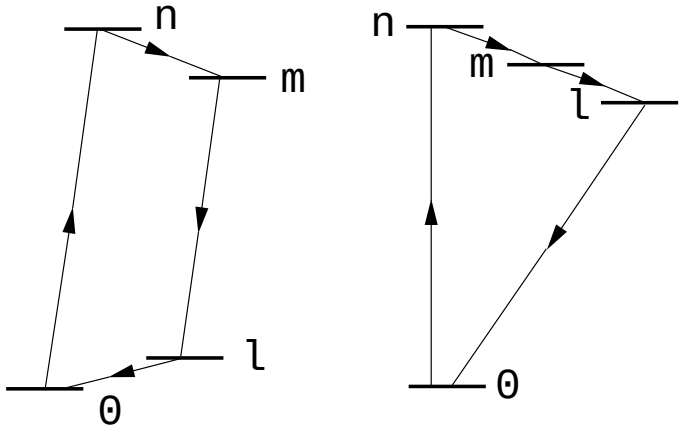

Figure 8

FIG. 8. Two possible four-link-chains.

The key observation is that the net transition amplitude (proportional to $\alpha_m(\nu)$) to go from $|0\rangle$ to a state $|m\rangle$ through degenerate intermediate states $|n\rangle$, $|l\rangle$, etc. is zero *unless there is a broken symmetry* leaving $\langle 0|\sigma_z|0\rangle \neq 0$. If the intermediate levels are degenerate, $\alpha_m(\nu)$ may be written

$$\alpha_m(\nu) = \sum_{n\neq 0,m} \frac{\sigma_{0n}\sigma_{nm}}{\nu-\nu_{n0}} = \frac{1}{\nu-\nu_{n0}} \sum_{n\neq 0,m} \sigma_{0n}\sigma_{nm} =$$

$$= -\frac{1}{\nu-\nu_{n0}}(\langle 0|\sigma_z|0\rangle\langle 0|\sigma_z|m\rangle + \langle m|\sigma_z|m\rangle\langle 0|\sigma_z|m\rangle) \qquad (29)$$

where the last line is obtained by inserting a complete set of states into $\langle 0|\sigma_z^2|m\rangle = 0$. Since the expectation value of σ_z is $O(1)$ only in the ground state (in the broken symmetry phase), we arrive at

$$\alpha_m(\nu) = -\frac{\langle 0|\sigma_z|0\rangle\langle 0|\sigma_z|m\rangle}{\nu-\nu_{n0}} = -\frac{\sigma_{00}\sigma_{0m}}{\nu-\nu_{n0}} \qquad (30)$$

Unless σ_{00} is non zero, the transition amplitudes for $|0\rangle \to |m\rangle$ involving an intermediate state interfere destructively. Finally, the integrated weight is obtained from (26),

$$I_{\rm nonlin} = {\rm const} \times \sum_{m\neq 0} |\alpha_m(\nu_{m0})|^2$$
$$= \frac{\rm const}{(\nu-\nu_{n0})^2} \times \sum_{m\neq 0} \sigma_{00}^2 \sigma_{0m}\sigma_{m0}$$
$$= \frac{\rm const}{(\nu-\nu_{n0})^2} \times \sigma_{00}^2(1-\sigma_{00}^2) \qquad (31)$$

where the sum rule (18) (with $j=0$) was used in the last line. This is the argument used to establish the result (27).

We now fill in the details of this argument appropriate for the numerical computation performed in this work by 1) setting $h_{\rm dc}=0$ and 2) including the finite width of the resonance. $\alpha_m(\nu)$ is to be evaluated at the frequency for TPA, $\nu=\nu_{m0}/2$—this frequency is about half of the typical frequencies of the intermediate levels ν_{n0}. α is rewritten in such a way as to separate the quasi-degenerate ground states from the excited states at the energy of the principal resonance at $O(t)$ (see Fig. 9):

$$\alpha_m(\nu_{m0}/2) = \frac{\sigma_{01}\sigma_{1m}}{\nu_{m0}/2-\nu_{10}} + \sum_{n\neq 0,1} \frac{\sigma_{0n}\sigma_{nm}}{\nu_{m0}/2-\nu_{n0}} \qquad (32)$$

$\nu_{10}=t^*\sim O(te^{-N/2})$ is the energy scale of the Franck-Condon resonance and will be set to zero. The difference between the resonant frequency, ν_{m0}, and the intermediate state level, ν_{n0}, which appears in the second term of (32) is bounded by the width of the primary resonance and is therefore typically much smaller than the primary resonance itself. Denoting a maximum value for that difference by ϵ (that is, $\nu_{n0}=\nu_{m0}+\epsilon$), the second term of (32) becomes:

$$\sum_{n\neq 0,1} \frac{-\sigma_{0n}\sigma_{nm}}{\nu_{m0}/2} + O(\frac{\epsilon}{\nu_0^2}) \qquad (33)$$

where ν_0 is the nominal energy scale of the resonance. Following the previous calculation for $h_{\rm dc}\neq 0$, the hyperpolarizibility α is now

$$\alpha_m(\nu_0) = \frac{4\sigma_{01}\sigma_{1m}}{\nu_0} + O(\frac{\epsilon}{\nu_0^2}) \qquad (34)$$

Substituting α back into equation (26) and using the sum rule (18) (with $j=1$) establishes the result (27).

To express $I_{\rm lin}$ and $I_{\rm nonlin}$ in terms of the control parameter κ, we appeal to the exact solution in the $N\to\infty$ limit. Specifically, the matrix element σ_{01} is related to the expectation value of σ_z in the either of the degenerate ground states of (4) (for $\kappa<\kappa_c$) by:

$$\lim_{N\to\infty} |\sigma_{01}| = |\langle\sigma_z\rangle_0| = \sqrt{\frac{1-\kappa^2}{1+\frac{\lambda^2}{\omega^2}\kappa^2}} = \sqrt{\frac{1-\kappa^2}{1+\frac{2t}{\omega}\kappa^2}} \qquad (35)$$

Therefore $I_{\rm lin}$ and $I_{\rm nonlin}$ may be compactly written in terms of κ:

$$I_{\rm lin} = \pi(\frac{1}{2})^2(1-\frac{1-\kappa^2}{1+\frac{\lambda^2}{\omega^2}\kappa^2}) \qquad (36)$$

$$I_{\rm nonlin} = \frac{2\pi h^2}{\nu_0^2}(\frac{1}{2})^4 \frac{1-\kappa^2}{1+\frac{\lambda^2}{\omega^2}\kappa^2}(1-\frac{1-\kappa^2}{1+\frac{\lambda^2}{\omega^2}\kappa^2}) \qquad (37)$$

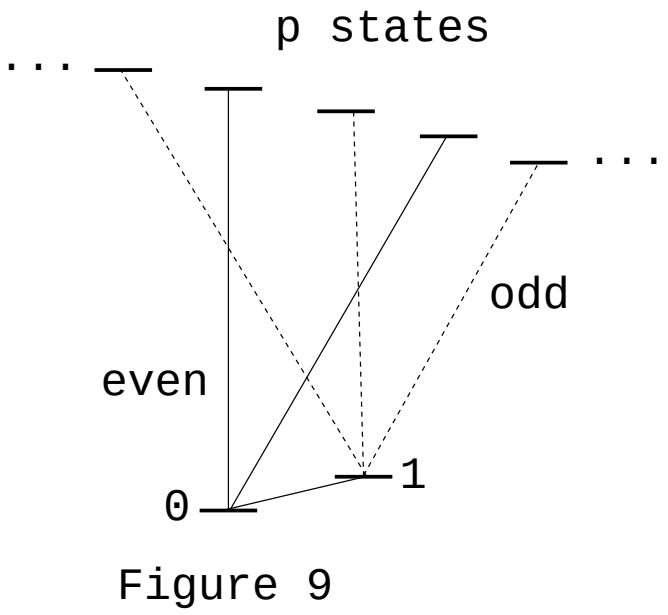

Figure 9

FIG. 9. Depiction of the quasi-degenerate ground state $|0\rangle, |1\rangle$ coupling to p excited states. The splitting between $|0\rangle, |1\rangle$ defining the Franck-Condon resonance is $O(te^{-N/2})$. The set of closely spaced excited states represents the inelastic broadening of the principal resonance.

Returning to fig. 7, the non-monotonic behavior of $I_{\rm nonlin}$ as a function of κ follows from its dependence upon the combination: $\langle\sigma_z\rangle^2(1-\langle\sigma_z\rangle^2)$. A plot of $I_{\rm nonlin}$ following from the analytic expression (37) is shown for comparison. In the numerical computations, the maximum intensity appears at approximately $\kappa=1/2$ in agreement with theory.

V. CONCLUSION

In this work we have attempted to make more explicit the relationship between the decoherence transition in the Mermin Model and a typical thermodynamic phase transition. At the onset of decoherence, spectral weight is transferred from above the "gap," set by the system energy scale t, to a delta function at $\nu=0$. This behavior is in contrast to the SBH where symmetry breaking is prefaced, first by the complete disappearance of the inelastic peak in $\chi''(\nu)$ at finite frequency (when $\alpha=1/2$), and then finally by the softening of renormalized system energy scale to zero (when $\alpha=1$).

Also, we have studied nonlinear absorption in a decoherent TLS. Single photon absorption is a measure of coherence of the system because it samples the spectral weight remaining at the principal resonance—or, the complement of the order parameter according to the sum rule. On the other hand, two-photon-absorption (TPA) samples the product of the order parameter and its complement and thus vanishes in the fully coherent or fully decoherent phase. TPA reaches maximum intensity somewhere between these two extremes.

Observing TPA may be possible in systems demonstrating quantum coherence such as the recently studied Fe_8 molecular nanomagnet. [9]. In principal, measurement of the ratio of $I_{\rm nonlin}$ to $I_{\rm lin}$ would provide a direct measure of the order parameter $\langle 0|\sigma_z|0\rangle$, the localized "weight" of the system. If we consider a sample in which the system spins are individually partially localized but uncorrelated with each other (like a spin glass), TPA may be a useful probe for this type of order.

ACKNOWLEDGMENTS

The author gratefully acknowledges the support of the Cottrell Foundation through Research Corporation Grant number CC3834. Work performed at BNL supported by the U.S. DOE under contract no. DE-AC02 98CH10886. The author also wishes to acknowledge many useful discussions with Dr. Jeffrey Clayhold, Dr. Barry Friedman, Dr. V. N. Muthukumar and the help of Joshua Eisner in performing some preliminary computations.

APPENDIX A: DERIVATION OF THE NONLINEAR DYNAMICAL SUSCEPTIBILITY

We begin by expressing the full time dependence of the expectation value of the desired operator in the presence of the driving field.

$$\langle\sigma_z(t)\rangle = \langle 0|U^\dagger(t,-\infty)\sigma_z(t)U(t,-\infty)|0\rangle \tag{A1}$$

where

$$\begin{aligned} U(t,-\infty) &= \mathbf{T}e^{-i\int_{-\infty}^{t}H(t')dt'} \\ &= 1 \underbrace{-i\int_{-\infty}^{t}dt_1 H(t_1)}_{I_1} \\ &\quad \underbrace{-\int_{-\infty}^{t}dt_1\int_{-\infty}^{t_1}dt_2 H(t_1)H(t_2)}_{I_2} \\ &\quad \underbrace{+i\int_{-\infty}^{t}dt_1\int_{-\infty}^{t_1}dt_2\int_{-\infty}^{t_2}dt_3 H(t_1)H(t_2)H(t_3)}_{I_3} \\ &\quad +\ldots \end{aligned} \tag{A2}$$

The time dependent operators appearing in these expressions are interaction picture operators, treating the full Hamiltonian (1) as the bare Hamiltonian and the external coupling Hamiltonian , $H(t) = -\frac{h}{2}\sigma_z(t)\cos\nu t$, as the perturbation. The S-matrix is expanded to the appropriate order. Grouping the third order terms in (A1) together, we arrive at:

$$\begin{aligned} &\langle 0|\sigma(t)I_3|0\rangle + \langle 0|I_3^\dagger\sigma(t)|0\rangle = \\ &\frac{-ih^3}{\hbar^3}\int_{-\infty}^{\infty}dt_1\int_{-\infty}^{\infty}dt_2\int_{-\infty}^{\infty}dt_3\langle 0|\sigma(t)\sigma(t_1)\sigma(t_2)\sigma(t_3)|0\rangle \\ &\times\cos\nu t_1\cos\nu t_2\cos\nu t_3\theta(t-t_1)\theta(t_1-t_2)\theta(t_2-t_3) \\ &+ \text{c.c.} \end{aligned} \tag{A3}$$

and

$$\begin{aligned} &\langle 0|I_1^\dagger\sigma(t)I_2|0\rangle + \langle 0|I_2^\dagger\sigma(t)I_1|0\rangle = \\ &\frac{+ih^3}{\hbar^3}\int_{-\infty}^{\infty}dt_1\int_{-\infty}^{\infty}dt_2\int_{-\infty}^{\infty}dt_3\langle 0|\sigma(t_1)\sigma(t)\sigma(t_2)\sigma(t_3)|0\rangle \\ &\times\cos\nu t_1\cos\nu t_2\cos\nu t_3\theta(t-t_1)\theta(t_1-t_2)\theta(t_2-t_3) \\ &+ \text{c.c.} \end{aligned} \tag{A4}$$

We use the integral representation of the step function,

$$\theta(t) = \frac{1}{2\pi i}\int_{-\infty}^{\infty}d\omega\frac{e^{i\omega t}}{\omega - i\delta}$$

($\delta = 0^+$) and collapse the time integrations. From the various products of delta functions, terms are grouped

according to whether they oscillate at $\pm 3\nu$ (third harmonic generation) or $\pm\nu$. From the latter terms, absorptive contributions come from the part of the signal that is $\pi/2$ out of phase with the driving term, $-\frac{h}{2}\sigma_z \cos\nu t$.

Terms that modify absorption at the original linear resonance, $\chi'' \sim P''_{n0}(\nu)$ can be grouped as follows:

$$\Omega_\gamma = \frac{1}{4}(\frac{h}{2})^4 \nu \frac{1}{\hbar^3} \sum_{nml} \sigma_{0n}\sigma_{nm}\sigma_{ml}\sigma_{l0} \times [P''_{0n}(-\nu)P'_{0m}(-2\nu)P'_{0l}(-\nu) + P''_{0n}(-\nu)P'_{0m}(0)(P'_{0l}(\nu) - P'_{l0}(\nu))] \quad \text{(A5)}$$

The two photon absorption terms can also be grouped as follows:

$$\Omega_{2\gamma} = \frac{1}{4}(\frac{h}{2})^4 \nu \frac{1}{\hbar^3} \sum_{nml} \sigma_{0n}\sigma_{nm}\sigma_{ml}\sigma_{l0} \times P''_{0m}(-2\nu)P'_{l0}(\nu)P'_{n0}(\nu) \quad \text{(A6)}$$

[1] See A. J. Leggett, S. Chakravarty, A. T. Dorsey, Matthew P. A. Fisher, Anupam Garg, and W. Zwerger, Rev. Mod. Phys. **59**, 1 (1987) and references therein.

[2] N. D. Mermin, Physica A **177**, 561 (1991).

[3] J. Shao and P. Hänggi, Phys. Rev. Lett. **81**, 5710 (1998).

[4] J. T. Stockburger and C. H. Mak, Phys. Rev. Lett. **80**, 2657 (1998).

[5] F. Lesage, H. Saleur and S. Skorik, Phys. Rev. Lett. **76**, 3388 (1996).

[6] M. Tinkham and R. A. Ferrell, Phys. Rev. Lett. **2**, 331 (1959).

[7] P. N. Butcher and D. Cotter, *The Elements of Nonlinear Optics* (Cambridge University Press, Cambridge CB2 1RP, UK, 1990).

[8] A. Garg, Phys. Rev. Lett. **74**, 1458 (1995); N. V. Prokof'ev and P. C. E. Stamp, J. Phys. Condens. Matter **5**, l663 (1993); "Spin Environments and the Suppression of Quantum Coherence," N. V. Prokof'ev and P. C. E. Stamp, chapter in *Quantum Tunneling of Magnetization*, ed. L. Gunther and B. Barbara, Kluwer Publishing (1995); G. Levine, Phys. Rev. **B56**, 1 (1997).

[9] E. del Barco, N. Vernier, J. M. Hernandez, J. Tejada, E. M. Chudnovsky, E. Molins and G. Bellessa, LANL e-print cond-mat/9810261.